

Spin-echo and Gradient-echo PWI CBF vs. ASL CBF: An Initial Comparison.

M. STRAKA¹, H. SCHMIEDESKAMP¹, G. ZAHARCHUK¹, J. B. ANDRE¹, J-M. OLIVOT², N. J. FISCHBEIN¹, M. G. LANSBERG², M. E. MOSELEY¹, G. W. ALBERS², AND R. BAMMER¹

¹RADIOLOGY, STANFORD UNIVERSITY, STANFORD, CA, UNITED STATES, ²STANFORD STROKE CENTER, STANFORD UNIVERSITY, STANFORD, CA, UNITED STATES

PURPOSE – SAGE PWI sequence [1, 2] leverages on both gradient-echo (GRE) and spin-echo (SE) data for advanced perfusion-weighted imaging (PWI). It also allows quantification of the baseline R_2 and R_2^* , as well as true ΔR_2 and ΔR_2^* changes during the passage of the gadolinium tracer. This sequence allows one to quantify perfusion parameters from both capillaries (via SE data) and arterioles/venules (via GRE data) at high temporal resolution and without T_1 contamination. Although current routine PWI scans use primarily the GRE data, it has been long suggested that cerebral blood flow (CBF) values derived from GRE are overestimated due to excessive sensitivity to larger vessels. Here, we compared CBF values from by GRE- and SE-based SAGE CBF to reference arterial-spin labeling (ASL) CBF data.

METHODS – Ten clinical cases were acquired using a 3T GE Discovery MR750 scanner. The study was IRB approved and written informed consent was obtained from each subject. ASL CBF datasets were acquired using a 3DFSE pseudo-continuous ASL sequence [3] (TR/TE/TL/PLD: 5500/2.5/1500/2000 ms) 10-20 minutes before the DSC-MRI. The DSC-MR PWI datasets were acquired using SAGE PWI sequence [1, 2]: multi-echo GRE and SE EPI with GRAPPA parallel imaging (R=3), TR=1.8s, 5 echoes, $TE_{GRE} = \{17, 34\}$ ms, $TE_{GRE} = \{62, 80\}$ ms, $TE_{SE} = 97$ ms, matrix 84², 15 slices (5mm thickness, 2mm gap), 60 time frames) with an injection of Gd tracer (Magnevist) of 0.1mmol/kg body weight @ flow rate of 4.5ml/s. Maps of quantitative perfusion parameters (including CBF and T_{max}) maps were determined via circular deconvolution [4]. Four types of CBF maps were computed: 1) using the 2nd GRE only ('single GRE'); 2) using the SE only ('single SE'); 3) using ΔR_2^* -based data; and 4) using ΔR_2 -based data. A non-linear correction for tracer effects in bulk blood and tissue was applied as outlined in [5], with an identical correction factor applied to both SE and GRE data (see Discussion). The ASL CBF maps were spatially coregistered with the PWI CBF maps. After resampling the ASL CBF maps into the SAGE coordinate space, non-brain regions (ventricles, scalp, large vessels, etc.) were semi-automatically removed. In first step of the analysis, the ASL CBF and the 4 types PWI CBF values were compared on a per-voxel basis. Thereafter, the PWI CBF values were rescaled in a way that the whole-brain medians of PWI CBF and ASL CBF values were identical. The scaling factors were derived from regions deemed to have normal blood flow [6], what has proven helpful to mitigate errors arising from AIF and VOF scaling. Gray and white matters were

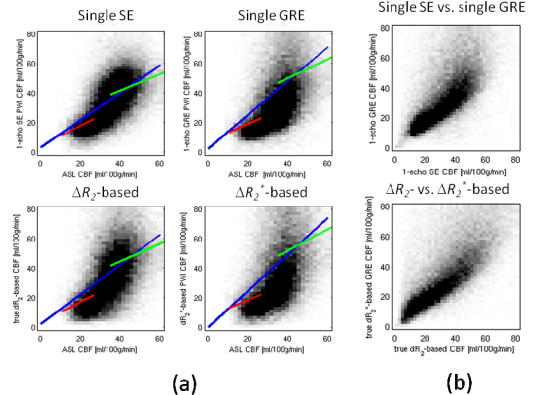


Fig. 1. Voxel-wise comparison between ASL and PWI CBF: (a) relation between ASL CBF & 4 types of SAGE PWI CBF values (upon normalization of median PWI CBF values to median ASL CBF). Blue is regression line for whole brain, red is regression line for white matter and green is regression line for gray matter (Tab. 2). (b) Relation of PWI CBF between SE and GRE data.

manually segmented by thresholding the ASL CBF.

RESULTS – Fig. 1a shows an example dataset out of the ten cases analyzed, demonstrating the relationship between ASL CBF and the 4 types of SAGE CBF values. Fig. 1b shows the relation between SE and GRE-based, as well as ΔR_2 and ΔR_2^* -based CBF values (using identical AIF and VOF). Tab. 1 summarizes the relation between ASL and PWI CBF for the whole brain, whilst Tab. 2 summarizes the same relation for gray and white matter separately.

DISCUSSION – Our initial results show that CBF derived from SE-based maps was approx. 4.8-times smaller than CBF derived from GRE-based maps (Tab. 1, col. 2), and hence the SE CBF must be corrected with this factor to match GRE CBF values. The 4.8-fold difference was very similar between gray and white matter (data not shown), and could be considered in future studies. Results also show that SE- and ΔR_2 -based CBF maps correlate with ASL CBF better than GRE or ΔR_2^* -based maps (Tab. 1, col. 4) as the large vessel contribution present on GRE-based maps tend to obfuscate tissue microperfusion. Our results also manifest that the slope of SE CBF vs. ASL CBF is less than 1.0, and the intercept is non-zero (Tab. 1 and Fig. 1a). Specifically, the relation between ASL CBF and SE CBF was different in both gray and white matter (Tab. 2), which is most likely caused by sensitivity of ASL to label delay and variable label efficiency in gray and white matter. Based on the correlation coefficient R (Tab. 1) and visual impression, we conclude that SE-based/ ΔR_2 -based PWI CBF maps are more similar to ASL than those obtained from single-GRE/ ΔR_2^* -based data. However, differences between single-SE and ΔR_2 -based data require further analysis.

Tab. 1. Summary of relation between ASL CBF and 4 types of PWI CBF values for the whole brain. Column 2 shows normalization factors necessary for ensuring identical whole-brain medians between ASL and PWI values. Column 3 is related to blue lines in Fig. 1a, and column 4 shows a measure of agreement between the ASL and PWI CBF values.

ASL vs. PWI CBF	Whole-brain CBF ratios before ASL/PWI normalization (median)	PWI/ASL slope after ASL/PWI normalization (median)	Correlation coefficient R (median)
Single GRE	2.1	0.92	0.35
Single SE	10.0	0.72	0.53
ΔR_2^*	2.2	0.99	0.35
ΔR_2	10.4	0.77	0.42

Tab. 2. Summary of the relation between ASL CBF and PWI CBF values in gray and white matter (upon normalization of median PWI CBF values to median ASL CBF). The whole brain median CBF was 35.5 ml/100g/min. Column 4 relates to red lines, and column 5 relates to green lines in Fig. 1a.

obtained from single-GRE/ ΔR_2^* -based data. However, differences between single-SE and ΔR_2 -based data require further analysis.

REFERENCES – [1] Newbould, RD. *et al.* Proc. ISMRM 2007. [2] Schmiedeskamp, H. *et al.*, Proc ISMRM 2010 p2962. [3] Dai *et al.*, MRM 2008, [4] Straka, M. *et al.* JMRI 2010(32): 1024-1037. [5] Kjølby, BV *et al.* MRM 2006(56): 187-197. [6] Zaharchuk, G. *et al.* MRM 2010.

ACKNOWLEDGEMENTS – NIH (5R01EB002711, 5R01EB008706, 3R01EB008706, 5R01EB006526, 5R21EB006860, 2P41RR009784, 1R01NS066506, 2R01NS047607-05), Lucas Foundation, Oak Foundation.